# Crystallization-induced stress in thin phase change films of different thicknesses

Qiang Guo,[1,2,a)] Minghua Li,[3,b)] Yi Li,[1,2] Luping Shi,[3] Tow Chong Chong,[3] Johannes A. Kalb,[1,4,c)] and Carl V. Thompson[1,4]
[1]*Singapore-MIT Alliance, 4 Engineering Drive 3, Singapore 117576*
[2]*Department of Materials Science and Engineering, National University of Singapore, 7 Engineering Drive 1, Singapore 117576*
[3]*Data Storage Institute, (A*STAR) Agency for Science, Technology and Research, DSI Building, 5 Engineering Drive 1, Singapore 117608*
[4]*Department of Materials Science and Engineering, Massachusetts Institute of Technology (MIT), Cambridge, Massachusetts 02139, USA*

(Received 12 September 2008; accepted 6 November 2008; published online 2 December 2008)

We have studied crystallization-induced stress in phase change films ($Ge_2Sb_2Te_5$) as a function of thickness and with and without a capping layer, by measuring the deflection of microcantilevers. The stress is found to increase with decreasing film thickness. A thin dielectric capping layer leads to a further increase in stress compared to uncapped films. This observation can be explained by the suppression of stress relaxation in the phase change film in the presence of a capping layer. High stress will affect device performance as the size of phase change memory cells decreases. © *2008 American Institute of Physics*. [DOI: 10.1063/1.3040314]

Recently, there has been an increasing industrial and academic interest in phase change random access memories (PCRAMs), which employ a thin film of a phase change material (usually an SbTe-based alloy) that is locally and reversibly switched between its crystalline and amorphous states using electrical current pulses.[1,2] The two states can subsequently be distinguished by their pronounced difference in electrical conductivity.[3–5] Due to their high speed and good scalability, PCRAMs are considered a promising alternative to current Flash memories.[1,2]

Phase change materials are characterized by a large volume change upon crystallization, ranging from 6% to 9%.[3,5,6] This could negatively affect the performance and reliability of phase change memories, decreasing, for example, the number of write/erase cycles the device can sustain.[7,10] If accommodated elastically, this volume change can result in a high film stress on the order of 1 GPa.[8,9] However, wafer curvature measurements have shown that the measured film stress is only 0.1–0.2 GPa,[10,11,14] implying that the majority of the stress relaxes plastically during crystallization. Although those studies (for which a thin phase change film was deposited on a relatively thick substrate) provide valuable insight into the stress buildup upon crystallization of continuous phase change films, they have limited significance for the stress buildup in phase change memory prototypes. In such devices, the memory cell is embedded in various abutting layers of metals and dielectrics.[12,13] Further, when memory cells are scaled down, the mechanical confinement applied to the phase change layer is expected to increase, making the crystallization-induced stress a more serious issue for device reliability.[14]

To qualitatively probe the different stress levels due to mechanical confinement that will occur in phase change layers in memory cells, we developed[15] and employed a new experimental method to measure the crystallization-induced film stress using microfabricated silicon nitride[16] (SiN) cantilevers. Amorphous phase change films of different thicknesses were deposited on those cantilevers. Upon heating-induced crystallization, the increase in density (i.e., decrease in volume) of the film makes the cantilevers deflect upwards, as a result of the tensile elastic mismatch strain developed at the interface between the film and the SiN cantilever. By comparing the magnitudes of the cantilever tip deflection before and after crystallization, the corresponding film stress can be determined accurately.[15,17,18] The ratio between the phase change film thickness and the SiN cantilever thickness ($=h_{GST}/h_{SiN}$, where $h_{GST}$ and $h_{SiN}$ are the thicknesses of the phase change and SiN layers, respectively) controls the mechanical constraint on volume changes in the phase change material. $Ge_2Sb_2Te_5$ (GST) was selected as the phase change material in this study, since it has been extensively studied and since it is a prototypical material in PCRAM test devices.[1]

$218 \pm 3$ nm thick low-stress SiN microcantilevers were fabricated through standard microprocessing techniques.[15] Phase change films of thicknesses ranging from 5 to 240 nm were then sputter-deposited on top of the cantilevers using a single target with a nominal composition of GST. Two sets of samples were prepared. In the first set, the GST layer was sandwiched between two thin layers (5 nm) of $ZnS(80)-SiO_2(20)$,[19,20] as schematically shown in Fig. 1. In the second set of samples, the GST films were directly deposited on the SiN beams, with neither capping nor underlayers. The GST film was deposited under a background pressure of $7 \times 10^{-7}$ mbar. The working pressure during sputtering was $5 \times 10^{-3}$ mbar, with an argon (Ar) flow rate of 20 SCCM (SSCM denotes cubic centimeter per minute at STP). The direct current sputter power was 100 W, leading to a deposition rate of about 0.86 nm/s. $ZnS-SiO_2$ layers were deposited under a working pressure of $4 \times 10^{-3}$ mbar with an Ar flow rate of 15 SCCM. The radio-frequency sputter

a)Electronic mail: guoqiang@mit.edu.
b)Electronic mail: li_minghua@dsi.a-star.edu.sg.
c)Present address: Intel Corporation, 2200 Mission College Blvd., Santa Clara, CA 95054, USA.

 

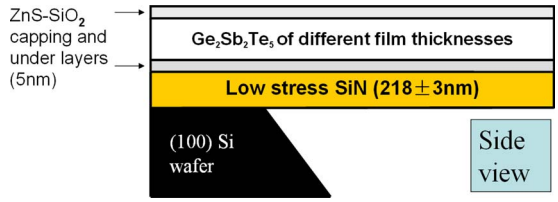


FIG. 1. (Color online) Layer structure of a microcantilever with a fixed support. A thin film of amorphous GST of various thicknesses was sandwiched between two thin (5 nm) layers of ZnS–$SiO_2$. The trilayer structure was deposited on a SiN cantilever (thickness 218±3 nm). Similar structures without ZnS–$SiO_2$ layers have also been fabricated for comparison. The thicknesses of the layers are not drawn to scale.

power was 1000 W, and the deposition rate was about 2.11 nm/s. As determined by x-ray diffraction (XRD), the structure of the as-deposited GST film was entirely amorphous. Subsequently, the samples were annealed in a furnace at 200 °C for 5 min in an Ar atmosphere. The temperature uncertainty was ±1 °C. The post annealing GST film structure was cubic as confirmed by XRD spectra.[4,6,21] The cantilever tip deflections before and after crystallization were measured with an optical profilometer (for small deflections) and/or an optical microscope (for large deflections).[15]

Figure 2(a) shows a top-view optical micrograph and the

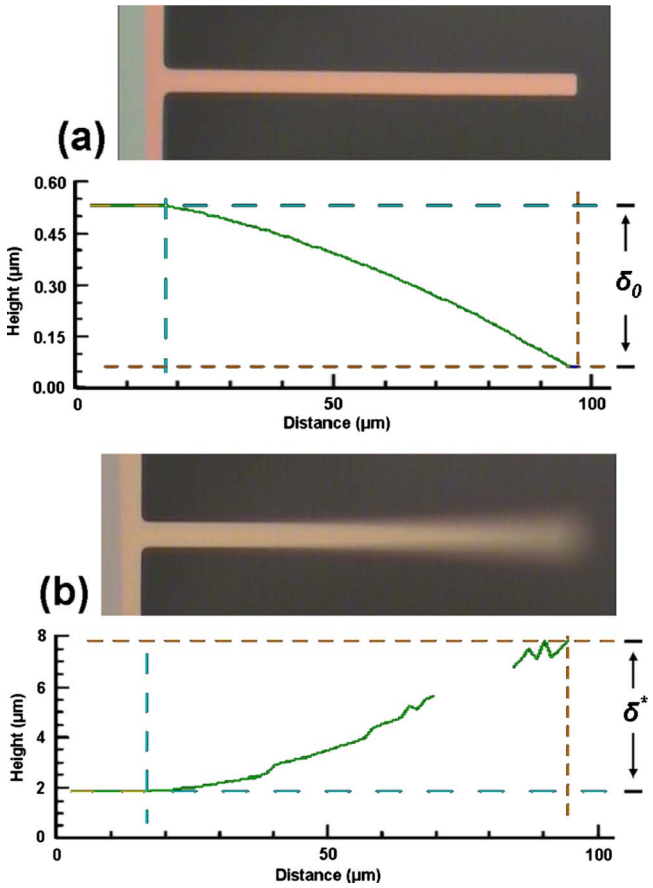


FIG. 2. (Color online) (a) Top-view optical micrograph (upper figure) and optical profilometry scan in side view (lower figure) of a 218 nm thick SiN cantilever onto which a 10 nm thick amorphous GST film has been deposited. The GST layer is sandwiched between 5 nm thick ZnS–$SiO_2$ capping and under layers. The cantilever is 80 $\mu$m long and 5 $\mu$m wide, and the tip of the cantilever is bent downwards to $\delta_0=-0.47\pm0.02$ $\mu$m. (b) Cantilever from (a) after furnace crystallization of the GST film. The cantilever is bent upwards by $\delta^*=5.95\pm0.05$ $\mu$m.

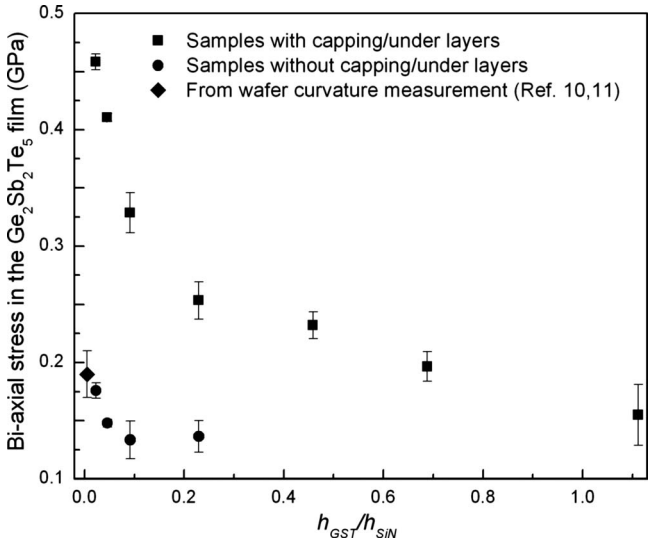


FIG. 3. Crystallization-induced stress in GST layers for different GST to SiN thickness ratios ($h_{GST}/h_{SiN}$). Tensile stress is defined to be positive. The filled squares are data points for the samples with ZnS–$SiO_2$ capping and under layers. Their corresponding GST film thicknesses are (from low to high) 5, 10, 20, 50, 100, 150, and 240 nm, respectively. The filled circles are data points for samples without capping and under layers. Their corresponding GST film thicknesses are (from low to high) 5, 10, 20, and 50 nm, respectively. Also shown in the figure is a data point from a previous wafer curvature measurement (see Refs. 10 and 11).

profilometer scan of an 80 $\mu$m long and 5 $\mu$m wide cantilever with ZnS–$SiO_2$ layers before GST crystallization. The corresponding GST film thickness is 10 nm. The profilometer scan reveals that the tip of the cantilever is slightly bent downwards to $\delta_0=-0.47\pm0.02$ $\mu$m. Crystallization induced an upward tip deflection of $\delta^*=5.95\pm0.05$ $\mu$m, as shown in Fig. 2(b). Using $\delta_0$ and $\delta^*$, the crystallization-induced mismatch strain and biaxial film stress in the GST layer can be calculated.[15,17,18] The mechanical properties of the films used in the calculations were $M_{SiN}=267\pm12$ GPa,[16,22] $M_{ZnS-SiO_2}=105\pm5$ GPa,[23] and $M_{GST}=45.2\pm8.2$ GPa,[9] where $M_{SiN}$, $M_{ZnS-SiO_2}$, and $M_{GST}$ are the biaxial moduli of the SiN, ZnS–$SiO_2$, and the GST layers, respectively.

Figure 3 shows the calculated[15] film stresses for several ratios of $h_{GST}/h_{SiN}$ for samples with and without capping/underlayers. For films that are *thick* compared to the SiN substrate, the film stress generally varies linearly through its thickness.[17] This effect (which can usually be neglected for very *thin* films[17]) has been accounted for in Fig. 3 by plotting the respective *average* GST stress for the three larger thickness values of $h_{GST}=100$, 150, and 240 nm, which correspond to $h_{GST}/h_{SiN}\approx0.46$, 0.69, and 1.11, respectively. Due to the linear variation,[17] the average is the arithmetic mean of the stress at the top film surface and the stress at the bottom film surface, both of which have been found to be positive (tensile). For the four smaller film thickness values, this effect has been found to be negligible, and therefore, the film stress was treated as a constant in the out-of-plane direction inside the phase change layer. In both sets of samples, the film stress increases as the phase change layer becomes thinner (lower $h_{GST}/h_{SiN}$ values), and the maximum measured stresses are about 0.46 and 0.18 GPa for the capped and uncapped films, respectively, both occurring at $h_{GST}=5$ nm ($h_{GST}/h_{SiN}\approx0.02$). As mentioned above, if the volume change upon crystallization were entirely elastically accom-

modated in the GST film, the film stress would be on the order of 1 GPa.[6,8,9] Therefore, since only elastic transformation induces a stress buildup, the observation illustrated in Fig. 3 indicates that for all GST thicknesses and for both (with and without capping layer) sample sets, a significant portion of the stress is relaxed plastically during crystallization, and this contribution decreases with decreasing film thickness.

Also shown in Fig. 3 are the film stress data from the previous wafer curvature measurement of $(190 \pm 20)$ MPa,[10,11] which is in good agreement with the experimental data in this work for films without capping/underlayers. Generally, the samples with capping layers exhibit a film stress that is about a factor of 2 higher than the films without capping layers. Indeed, it has been reported that the good adhesion between the capping layer to the phase change film prevents fluidization and flow of the film during the heating process.[19,24,25] Therefore, the capping layer might constrain mechanical creep associated with surface diffusion in the crystalline film.[26] Those effects could possibly lead to a reduction in the amount of stress relaxation.

Since the measured stress in the GST films is related to the elastically accommodated portion of the total volume change upon crystallization,[15] it can provide a measure of the yield stress of the films.[30] In phase change materials, the stress relaxation during crystallization is likely to occur in the amorphous phase.[10] Thus, the data in Fig. 3 imply that the yield stress of the amorphous GST film increases with decreasing film thicknesses. Earlier studies have shown that amorphous metals have a significantly larger yield stress when the sample dimension is reduced.[27,28] It was argued that, in smaller samples, the defect population is lowered, resulting in an improved materials strength.[27–29] In addition, it is also known that the yield stress of polycrystalline films increases when the films become thinner.[30–32] This is because the driving force for the dislocation nucleation and propagation decreases with decreasing film thickness, making the stress relaxation process (yield of the film) less energetically favorable, so that a larger measured (elastically accommodated) stress is expected. Our results further support the general principle that increasing materials strength (yield stress) with decreasing sample dimensions is probably also valid for amorphous semiconductor films (GST in this study).

In conclusion, the measured stress upon crystallization of amorphous GST phase change films that are deposited on microcantilevers increases when volume changes are increasingly mechanically constrained. This phenomenon can be explained in terms of a yield stress of the phase change layer that depends on the layer thickness. Additionally, it was found that a thin capping layer has a profound effect in suppressing stress relaxation in the phase change film. Compared to simple wafer curvature measurements,[10,11,14] our findings enable more precise modeling of write/erase-induced stress buildup in phase change memory cells, in which the phase change materials have small dimensions and are mechanically constrained by surrounding material. This will allow better predictions of device performance and reliability and lead to the design and implementation of improved cell geometries.

The Data Storage Institute (DSI) of Singapore supported the NUS-DSI component of this research and the Singapore-MIT Alliance (SMA) supported the MIT component of this research. Q.G. was also supported by an SMA Fellowship and J.A.K. was partially supported by the Alexander-von-Humboldt Foundation. We thank C. Sow for help with optical microscopy and H. Yu for help with the optical profilometry.

[1] S. Hudgens and B. Johnson, MRS Bull. **29**, 829 (2004).
[2] M. H. R. Lankhorst, B. W. S. M. M. Ketelaars, and R. A. M. Wolters, Nat. Mater. **4**, 347 (2005).
[3] D. Wamwangi, W. Njoroge, and M. Wuttig, Thin Solid Films **408**, 310 (2002).
[4] I. Friedrich, V. Weidenhof, W. Njoroge, P. Franz, and M. Wuttig, J. Appl. Phys. **87**, 4130 (2000).
[5] W. Njoroge and M. Wuttig, J. Appl. Phys. **90**, 3816 (2001).
[6] W. Njoroge, H. Wöltgens, and M. Wuttig, J. Vac. Sci. Technol. A **20**, 230 (2002).
[7] S. H. Hong and H. Lee, Jpn. J. Appl. Phys. **47**, 3372 (2008).
[8] U. Laudahn, S. Fähler, H. U. Krebs, A. Pundt, and M. Bicker, U. v. Hülsen, U. Geyer, and R. Kirchheim, Appl. Phys. Lett. **74**, 647 (1999).
[9] J. Kalb, F. Spaepen, T. Pedersen, and M. Wuttig, J. Appl. Phys. **94**, 4908 (2003).
[10] T. Pedersen, J. Kalb, W. Njoroge, D. Wamwangi, M. Wuttig, and F. Spaepen, Appl. Phys. Lett. **79**, 3597 (2001).
[11] J. Kalb, MS thesis, Rheinisch-Westfälische Technische Hochschule (RWTH), Aachen, Germany (2002).
[12] G. F. Zhou, Mater. Sci. Eng., A **304**, 73 (2001).
[13] H. J. Kim, S. K. Choi, S. H. Kang, and K. H. Oh, Appl. Phys. Lett. **90**, 083103 (2007).
[14] L. Krusin-Elbaum, C. Cabral, Jr., K. N. Chen, M. Copel, D. Abraham, K. Reuter, S. Rossnagel, J. Bruley, and V. Deline, Appl. Phys. Lett. **90**, 141902 (2007).
[15] J. A. Kalb, Q. Guo, X. Zhang, Y. Li, C. Sow, and C. V. Thompson, J. Microelectromech. Syst. **17**, 1094 (2008).
[16] H. Guo and A. Lal, J. Microelectromech. Syst. **12**, 53 (2003).
[17] S. Suresh and L. Freund, *Thin Film Materials—Stress, Defect Formation and Surface Evolution* (Cambridge University Press, Cambridge, 2003), Chap. 2.
[18] L. Freund, J. Floro, and E. Chason, Appl. Phys. Lett. **74**, 1987 (1999).
[19] N. Ohshima, J. Appl. Phys. **79**, 8357 (1996).
[20] E. R. Meinders, H. J. Borg, M. H. R. Lankhorst, J. Hellmig, and A. V. Mijiritskii, J. Appl. Phys. **91**, 9794 (2002).
[21] J. Kalb, F. Spaepen, and M. Wuttig, J. Appl. Phys. **93**, 2389 (2003).
[22] S. Senturia, *Microsystems Design* (Kluwer Academic, Boston, MA, 2001), p. 196.
[23] D. V. Tsu and T. Ohta, Jpn. J. Appl. Phys. **45**, 6294 (2006).
[24] W. Njoroge, H. Dieker, and M. Wuttig, J. Appl. Phys. **96**, 2624 (2004).
[25] A. Ebina, M. Hirasaka, J. Isemoto, A. Takase, G. Fujinawa, and I. Sugiyama, Jpn. J. Appl. Phys. **40**, 1569 (2001).
[26] M. D. Thouless, J. Gupta, and J. M. E. Harper, J. Mater. Res. **8**, 1845 (1993).
[27] C. J. Lee, J. C. Huang, and T. G. Nieh, Appl. Phys. Lett. **91**, 161913 (2007).
[28] B. E. Schuster, Q. Wei, M. Erwin, S. Hruszkewycz, M. Miller, T. Hufnagel, and K. Ramesh, Scr. Mater. **57**, 517 (2007).
[29] M. Ashby and D. R. H. Jones, *Engineering Materials 2: An Introduction to Microstructures, Processing and Design* (Pergamon, Oxford, 1986), Chap. 18, pp. 169–170.
[30] R. Venkatraman and J. Bravman, J. Mater. Res. **7**, 2040 (1992).
[31] M. Hommel and O. Kraft, Acta Mater. **49**, 3935 (2001).
[32] W. Nix, Metall. Trans. A **20**, 2217 (1989).